Polímeros
ISSN 1678-5169 (Online)

https://doi.org/10.1590/0104-1428.20220110

ORIGINAL ARTICLE

Thermodynamics of the polymerisation of polyglycerols in an acidic and micellar environment

Vadilson Malaquias dos Santos[1], Fabricio Uliana[1], Rayanne Penha Wandenkolken Lima[1] and Eloi Alves da Silva Filho[1*]

[1]Laboratório de Físico-química, Departamento de Química, Universidade Federal do Espírito Santo – UFES, Vitória, ES, Brasil

**eloisilv@gmail.com*

Abstract

This work consisted of studying polyglycerols in an acidic and micellar environment. The effects on surface tension, micellisation, and the Gibbs free energy of interface liquid-liquid (w/o) for directing the etherification of monomer glycerol with n-hexanol, n-octanol, n-decanol, n-dodecanol, and micellar solutions of sodium dodecylsulfate and dodecylbenzenesulfonic acid were studied at 70, 90 and 130°C . Polyglycerols with low weights and prepolymers were obtained. Theoretical methods such as density functional theory and molecular dynamics simulations were used to examine the effects of surface tension, the conformations of glycerol, and the position of the hydroxyl group of alcohols. A theoretical analysis (DFT/B3LYP) of the potential energy surface of glycerol and alcohols allowed finding stable conformations of the molecule, differing in the relative arrangement of hydroxyl groups. Our results helped achieve a better understanding of the interaction complex process of surfactant/catalyst of glycerol reactions in biphasic systems.

Keywords: *hydroxyl groups, liquid systems, surfactants.*

How to cite: Santos, V. M., Uliana, F., Lima, R. P. W., & Silva Filho, E. A. (2024). Thermodynamics of the polymerisation of polyglycerols in an acidic and micellar environment. *Polímeros: Ciência e Tecnologia*, 34(1), e20240003. https://doi.org/10.1590/0104-1428.20220110

1. Introduction

Polyglycerols (PGs) are highly biocompatible and multifunctional polymers prepared from dicarboxylic acids, alcohols, or diols, which have a wide range of applications in the fields of pharmaceutics, biomimetic materials, foods, cosmetics, and catalysts[1-4]. The (1,2,3-propanetriol) glycerol (GLY) is completely soluble in water and numerous alcohols; it has three hydroxyl groups and is a highly flexible molecule which can form both intramolecular and intermolecular hydrogen bond networks, and its conformation (α, β, and γ) depends on variations in temperature and/or pressure[5]. The high viscosity and hydrophilicity of GLY and its selectivity resulting from the homo- or hetero- etherification of aliphatic alcohols cause the low yield of direct etherification and polymerization[6-8]. The Brønsted Acid-Surfactant-Combined Catalysed reactions of GLY have been shown to represent an excellent process capable of efficiently promoting the reaction of GLY under liquid/liquid biphasic system conditions[7-12]. Several studies in the literature have considered the performances of dodecylbenzenesulfonic acid (DBSA) for catalysis in biphasic water/oil (w/o) mixtures[11,12]. In comparison, sodium dodecylsulfate (SDS) is a surfactant exhibiting sulfonic sites which can also operate at the water/oil interface[12]. The properties of micelle formation and reduction of the surface tension in aqueous solutions gives surfactants excellent catalyst properties for the synthesis of PGs, in particular, because of the formation of microemulsions during the reaction[13-17]. As an alternative, non-ionic admixtures of surfactants and fatty alcohols, i.e., aliphatic hydrocarbons containing a hydroxyl group usually in the terminal or n-position (range C_6-C_{35}) affect the catalytic activity of polymerisation[18,19].

In this paper, experimental and theoretical methods were applied to study the effects of on surface tension, micellisation, molecular conformation, and Gibbs free energy of w/o interfaces; a synthetic strategy was used to prepare PGs through the direct etherification of GLY with alcohols using heterogeneous interfacial acidic catalysts and surfactants, SDS and DBSA, in the presence of acid cocatalysts.

2. Materials and Methods

2.1 Chemicals

The surfactants and other compounds used included DBSA (Sigma-Aldrich), SDS (Sigma-Aldrich), GLY (Sigma-Aldrich), sulfuric acid (Merk), chloridric acid (Sigma-Aldrich), acetic acid (Sigma-Aldrich), zinc chloride (Sigma-Aldrich), copper oxide (Sigma-Aldrich), potassium hydroxide (Merk), pyridine (Merk), 1-hexanol (HEX1; Vetec), 1-octanol (OCT1; Merk), 1-decanol (DEC1; Merk), and 1-dodecanol (DO1; Vetec).

2.2 Polymerization procedure

Mixtures of 1:1 (m/m) SDS and HCl and 1:1(m/m) SDS and $ZnCl_2$ were placed into a mortar where the mixture was ground for 5 min and allowed to stand for 10 min. A mixture of DBSA (32.6 g) and copper oxide (7.96 g) with a 1:1 molar ratio was added into a 100 mL three-neck flask and separated over 30 min at room temperature; the mixture was stirred at 25ºC, slowly heated to 110ºC, and kept at this temperature for 3 h in order to remove the water formed during the reaction process. The reaction was then cooled to 25 ºC. An equimolar mixture of GLY, aliphatic alcohols (HEX1, OCT1, DEC1, and DO1) and 5, 10, 15, and 20 mol% DBSA, DBSA/copper oxide, SDS/HCl, and water/SDS/$ZnCl_2$ catalysts, respectively, were added to a 50 ml single-necked round-bottom flask with a reflux condenser. The reaction mixture was continuously stirred using a magnetic stirrer for 20-24 h at room temperature or heated slowly to 70, 90, and 130ºC. A semisolid or solid was obtained which was filtered off, thoroughly washed with water, and dried in vacuum. For the water/GLY/alcohol system, an equimolar GLY was added to 50 mL of deionised water and 30 mol% DBSA and for the DBSA/copper oxide or SDS/HCl, water/SDS/$ZnCl_2$, respectively in a 200 mL of erlenmeyer flask with stirring at 80 ºC, after, added an equimolar aliphatic alcohols. The reaction mixture was then continuously stirred again using a magnetic stirrer for 20-24 h at heated slowly to 80, 90, and 130ºC.

2.3 Surface tension and critical micelle concentration (CMC) measurements

Surface tensions were measured using a Lauda TD3 tensiometer equipped with a Pt-Ir du Nouy ring at 25 ± 0.2ºC. All measurements were performed using solutions over a range of temperatures (25−65ºC). Specific conductivity data were measured with a conductometer to determine the critical micelle concentration (CMC) of the surfactant solutions. All the water was deionised.

2.4 Characterisation methods

DSC thermograms were recorded on a DSC Q200 (TA instruments). The samples were first cooled down to −80 ºC and then heated to 300 ºC at a ramping rate of 5 ºC/min. The DSC was used under an N_2 atmosphere to determine the glass transition temperature (Tg) and the temperature program equilibration was performed at T = −80 ºC. The first scan was performed to eliminate the thermal history of the polymers and remove volatile substances. A second heating cycle up to 300 ºC was completed at a rate of 5 ºC/min. The FTIR spectra were recorded on a FTLA 2000-102 (ABB Bomen) in the range between 4000-500 cm^{-1}. The hydroxyl value of the PGs was determined according to ASTM D4274-11[4]. The hydroxyl numbers of PGs were determined by measuring the free hydroxyl groups of the PGs acetylated with a solution of acetic anhydride- pyridine in a pressurised bottleat 98ºC, and the acetic acid was titrated with a 1.0 mol/L standard solution of potassium hydroxide (KOH). Viscosity was measured on a Rheotek RPV-1 viscometer at 25 ºC. The molecular weight of the PGs is measured by using viscometer technique.

2.5 Computational details

The structures of all the reactants and surfactants were generated manually using the Avogadro program[20]; these structures were initially optimised with the semi-empirical Hamiltonian PM7 using MOPAC2016 program[21] while the minimum energies and frequency calculations were re-optimised with density functional theory (DFT) calculations considering the B3LYP hybrid functional, with a 6-31G(d) basis set, DEF2-TZVP level of theory in the gas phase, and wb97X-D3 def2-SVP in the aqueous phase . All DFT calculations were carried out in vacuum and aqueous phase using the Orca 5.0.3 package[22]. The natural bond orbital (NBO) populations, frontier molecular orbital (FMO) properties, second-order perturbation stabilisation energies, dipole moments, and Fukui reactivity functions were further investigated using DFT while the molecules/system were prepared using the LigParGen web server[23], ACPYPE software[24], and PACKMOL software version 18.169[25]. The SPC and TIP3P models were applied for water[26]. All molecular dynamics (MD) simulations were performed with the GPU code of the GROMACS 2022.2 package, OPLS-AA force field[27]. The MD simulations of the liquid–liquid interface of the GLY/DO1 and water/DO1 systems were performed on the canonical (N, V, T) ensemble using a Nosé-Hoover thermostat set at a temperature of T = 22 ºC. The pressure tensor method was used to compute the interfacial tension, with the interface positioned perpendicular to the z-axis[15].

3. Results and Discussions

Glycerol and longer-chain alcohols are considered molecules that can form insoluble monolayers, thereby limiting mass transfer in reactions. The protonation of GLY is the first step in acid-catalysed oligomerisation, on the three reactive sites to accept a proton (two α sites and one β site) or three possible structural arrangements of the CH_2OH and OH groups: α, β, and γ[5,7,28,29]. This leads to the formation of diglycerol and tri-glycerol through the reaction of two or three GLY molecules (Figure 1A for molecules (6), (7), and (8)), and tri-glycerol through the reaction of two or three GLY molecules through primary hydroxyl. The direct etherification of DO1 and GLY produced hetero-ethers and homo-ethers (Figure 1B, molecules (10) and (11)) which are surface-active reagents[29]. Figure 2 shows the scheme of polymerisation of GLY in the presence of surfactants/water and surfactant-combined catalysts for 10 mol% of DBSA in a biphasic medium stirred at 130°C for 24 h. A monophasic system was observed for up to 20 mol% of DBSA. These results suggest that the stability of the emulsion, the temperature, and the interface contact are import factors for the formation of monomers. GLY/DO emulsions are unstable at high temperatures (~150°C). The results of the synthesis were in good agreement with those obtained in the literature for other similar synthesis procedures using a DBSA combined-catalyst[17,29,30]. The catalytic activity of the SDS is equivalent to that of the Brønsted acids and greater than that of most Lewis acids ($SnCl_4.6H_2O$, $FeCl_3.6H_2O$, and $LnCl_3.6H_2O$). In fact, SDS can hydrolyse into acid and alcohol under acidic conditions[31,32]. Moreover, SDS lowers the interfacial tension between phases to produce a transparent microemulsion and increases the effectiveness of a cocatalyst[33,34].

3.1 Polymers characterization

The synthesis produced low molecular weight PGs prepared of up to range 2,500-3,880 g/mol and the hydroxyl numbers of the polymers[4] obtained from the polymerisation of GLY ranged from 684 to 920 mg KOH/g (Table 1). PGs are colorless to yellowish solids and semisolids at room temperature (Figure 3).

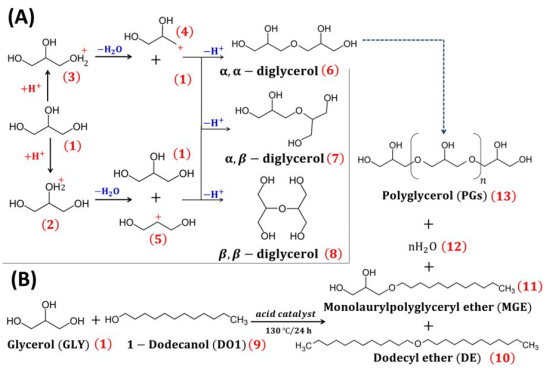

Figure 1. Reaction networks for the catalytic etherification of glycerol in acid medium (A) Homogeneous acid-catalyzed dimerization of glycerol. Adaptad of Valadbeigi and Farrokhpour[28]; (B) Direct etherification and polymerization of dodecanol and glycerol. Adaptad of Gaudin et al.[29] and Fan et al.[30].

Fourier transform infrared spectroscopy (FTIR) was used to identify the functional groups in the synthesised PGs (Figure 4). The PGs spectra showed the presence of hydroxyl group bands from 3050 to 3600 cm^{-1} indicative of alcohol groups. The absorption band at 1700–1750 cm^{-1} was related to C=O stretching due to the presence of acrolein (C_3H_4O) while the band at 2891 cm^{-1} was associated with aliphatic C-H. The peak at 1455 cm^{-1} that corresponded to C-OH in-plane bending and CH_2 bending, and the absorption at 1000–1150 cm^{-1} were related to the C-O stretching of the ether groups within the PG backbone. For polyglycerol PG1, the absorption ranging from 1734 to 1176 cm^{-1} was related to the C=O and C-O of ester groups, while C-H stretching produced bands ranging from 2875 to 2950 cm^{-1} (sp3). Polyglycerols, on the other hand, show three intense peaks at 3300, 2891, and 1100 cm^{-1} corresponding to the hydroxyl (OH), aliphatic C–H, and C–O bonds[29-32].

The thermal behaviour of the synthesised PGs was characterised by differential scanning calorimetry (DSC). The measurements of the thermal decomposition of the polymers allowed us to evaluate the temperature dependence of the PGs backbone structures.

DSC measured a melting temperature (Tm) during heating. Figure 5 plots the results for the PG1, PG2, and PG3. The Tg is observed as a slightly discernible step in the curves between –69.7, –42.8, and –16.5 °C. A melting transition is observed for PG1 at approximately –45.9 °C and, 2nd at 50.5 °C. The cold crystallisation took place at 1.8 °C.

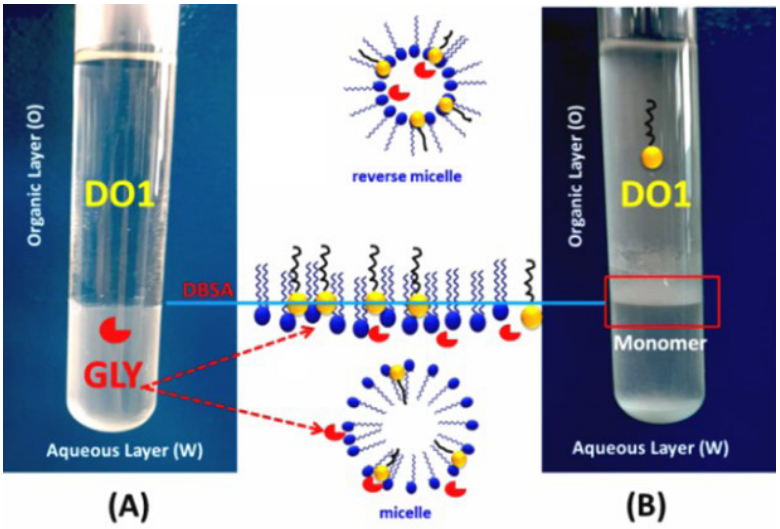

Figure 2. Concept of biphasic catalysis using surfactants (DBSA and SDS). (A) Start reaction, micelle and reverse micelle occupation by GLY and DO1; (B) Stabilize glycerol/dodecanol emulsions and low monomer prepolymer of polyglycerol.

Table 1. Properties of polyglycerols synthesized.

Name	Reaction conditions	Molecular weight (g/mol)	Viscosity (mPa.s) 20 °C	hydroxyl value (mg.KOH/g)
GLY	Pure	92	1,412	1,829
PG1	DBSA/DO1/H^+/130ºC/24h	3,880	10,893	684
PG2	SDS/OCT1/H^+/$ZnCl_2$/70ºC/20h	2,556	7,730	903
PG3	SDS/DO1/H^+/$FeCl_2$/90ºC /24h	3,280	9,893	920

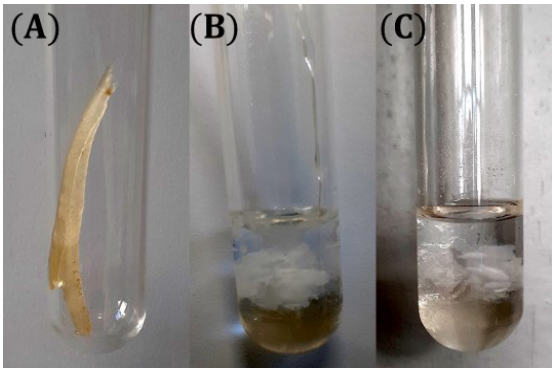

Figure 3. Image of a PGs (A) ellipsoids form of PG1 (B) interfacial semisolid of PG2 (C) semisolid aggregates of PG3.

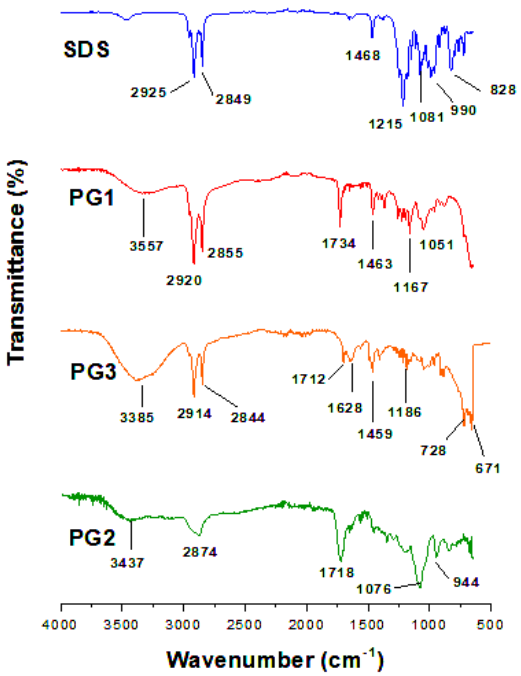

Figure 4. FTIR spectra of SDS, polyglycerol (PG1) and polyglycerol monomers (PG2 and PG3). The main peaks associated with the structures are highlighted.

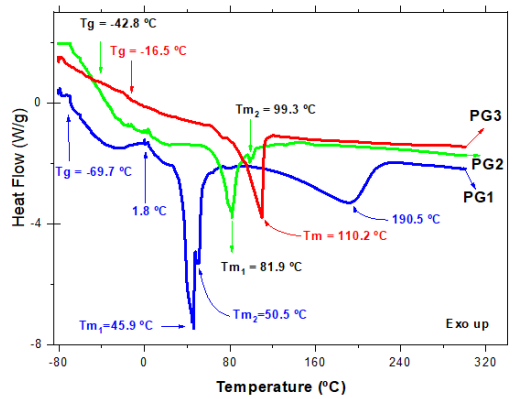

Figure 5. DSC curves for polyglycerol PG1, PG2 and PG3 thermal decomposition at a rate of 5 ºC/min.

The peak at 190.5 °C is relative to thermal degradation. The trend noted for the endothermic melting transition of PGs as temperature increases is a narrowing of the transition region for PG2 and PG3, a reduction in peak magnitude, and a general shift of the peaks towards high temperatures. The presence of endothermic peaks indicates that the PGs samples are semi-crystalline. The relative differences in a sample's degree of crystallinity can be quantified by measuring the relative differences between areas under the melting peaks. (ΔH_m) was calculated as the area under the peak by numerical integration: PG1 (80.57 J/g), PG2 (44.30 J/g), and PG3 (71.59 J/g).

3.2 Surface tension and CMC

The effect of alcohols on the interfacial tension can be described by their co-adsorption with surfactants in a mixed adsorption layer. The interfaces of the liquid-liquid system and the CMC are essential to the polymerisation of PGs, as they are often considered to be active sites for phase-transfer catalysis. All measurements of the surface tensions and CMC of the liquid-liquid systems, each in contact with surfactants, were performed over the same range temperature (25-65ºC). The specific conductance of SDS or DBSA changes with the total surfactant concentration and with temperature[35-37]. The values of CMC were obtained from the intersection of the two lines extending from the 'before micellisation' and the 'micellar' phase for all the considered temperatures. For SDS at 25ºC, the CMC was 7.01mmol/L and at 65ºC it was 9.91 mmol/L; for DBSA, the CMC was 37.5 mmol/L at 20ºC and 39.0 mmol/L at 50ºC. The CMC of SDS decreased from 7.01 to 6.05 mmol/L with the addition of zinc chloride due to the insertion of a counter ion between the surfactant molecules. In the same way, iron (II) chloride was highly soluble in water(64.4g/100 mL at 10°C), alcohol, and acetone, affecting the CMC of SDS. Copper (II) oxide was insoluble in water, GLY, and alcohols, acting as solid base catalyst for the reaction of GLY etherification[35]. The CuO did not reduce the interfacial tension of the system because it was not charged.

The aggregation number $n = (2.5229) l^3 \Delta d$ was calculated for all the temperatures considered, where $l = 1.5 + 1.265 n_c A^0$ is the length of the hydrocarbon chain attached to the head group, n_c is the number of carbon atoms attached to the hydrocarbon chain, and $\Delta d = d_2 - d_1$ and d_i are the densities of the water or oil solvent and surfactant solutions, respectively[37]. The degree of micellar ionisation ($\alpha = S_2 / S_1$) was taken as the ratio of the slopes of the straights (S_1;S_2) with inflection in CMC[37]. The degree of counterion binding ($\beta = 1 - \alpha$), α, CMC, aggregation number and surface tension are listed in Table 2 and 3. The Gibbs free energy of micellisation (ΔG_{mic}) could be approximated with Equation 1.

$$\Delta G_{mic} = \Delta H_{mic} - T\Delta S_{mic} = (2 - \alpha) RTln[CMC] \qquad (1)$$

In the plot showing ΔG_{mic} versus temperature, the slope was defined as $-\Delta S^0_{mic}$ and the intercept was equal to ΔH^0_{mic}[36]. For SDS, 25ºC, $\Delta G^0_{mic} = -20.6$KJ / mol, $\Delta H^0_{mic} = -36.4 KJ / mol$ and $\Delta S^0_{mic} = -0.032$KJ / mol. Table 4 lists the data obtained for the DBSA and SDS solutions and the w/o interface. The

Table 2. The degree of counterion dissociation (α) and binding (β) from/to the micelles and the slopes (S_1;S_2), CMC and aggregation number (n) for SDS.

Isotherm (ºC)	CMC (mmol/L) ± 0.5	S_1	S_2	α ± 0.02	β	n
25	7.20	67991	22041	0.324	0.676	69.02
35	7.72	63987	23281	0.364	0.636	64.20
45	8.32	67244	25268	0.378	0.624	55.10
55	8.93	67833	31985	0.471	0.528	47.63
65	9.91	68996	30839	0.447	0.553	40.11

Table 3. The degree of counterion dissociation (α), binding (β) and CMC from/to the micelles and the slopes (S_1;S_2), CMC and aggregation number (n) for DBSA.

Isotherm (ºC)	CMC (mmol/L) ± 0.3	S_1	S_2	α ± 0.04	β	n
10	36.9	276.0	551.9	0.50	0.50	104
20	37.5	397.0	554.0	0.72	0.28	98
30	37.8	464.9	562.8	0.82	0.18	93
40	38.6	384.8	577.3	0.66	0.34	87
50	39.1	520.5	598.8	0.87	0.13	82

Table 4. Surface tension (mN/m) data obtained with DBSA, SDS and interface water/oil*.

Temperature (ºC)	Water	Water/SDS	Water/DBSA	Interface tension
25	71.9	33.5	41.5	29.0
35	74.1	32.6	30.4	28.7
45	68.7	32.6	32.1	17.6
55	67.1	31.9	32.7	17.4
65	65.3	31.5	31.8	16.2
70	64.5	31.4	32.5	15.8

*w – water; o – dodecanol. Error: ±0.5 mN/m.

Table 5. Surface tension (mN/m) of binary organic-water systems and mixture**.

System	Pure	SDS	SDS/GLY	SDS/PGs	PG/GLY	PG
Water/HEX1	18.76	29.59	18.38	16.29	16.05	15.32
Water/OCT1	19.0	18.5	19.2	18.4	19.2	20.5
Water/DO1	29.0	33.5	24.1	23.0	29.3	28.4

**25 ±0.2ºC, Concentration: SDS 8 mmol/L; PG 0.2 g/mL. Volume: GLY 9.5 mL; alcohol 20.0 mL; water 20.0 mL. Error: ±0.5 mN/m.

initial interfacial tension of water at 20 °C was measured as 71.9 mN/m, which was very close to the value suggested in the literature (72 mN/m). The interfacial tensions between SDS and water, DBSA and water, and DO1 and water may also need to be confirmed (Table 4). The effects of SDS, GLY, and PG in aqueous solution on the initial interfacial tensions for three water-organic systems is provided in Table 5. Pure GLY had a surface tension of 63.4 mN/m at 20 °C. The interfacial tension had a value of 35.4 mN/m for GLY (20 wt%) and SDS (0.2 wt%) at 20°C. Fatty alcohols are insoluble in water and in the absence of salt, alcohol always reduces the surfactant aggregation number in the mixed surfactant/alcohol micelles, even with long-chain alcohols such as HEX, OCT, and DO[38,39].

3.3 Theoretical study

In aqueous environments, asymmetric alcohols where the hydroxyl group is not located at a chain, and which lack any symmetry elements – except for the identity operation (C_1) – will preferentially form monolayers at the water/vapour interface, which interferes with the catalytic process of PGs[40]. Figure 6A shows the optimised structures of alcohols with the minimum energy obtained through the DFT method; only the structures of DO conformers (*g*, gauche and *t*, trans) obtained with B3LYP/6-31G(d) in a gas phase are presented. However, no significant differences were observed when comparing these structures with the DFT/B3LYP/6-31G and wb97X-D3 def2-SVP in water. For instance, the main differences observed were in angle of the attached C−OH groups (Figure 6B). Figure 6C shows the molecular electrostatic potential (MEP) obtained from NBO atomic charges at the wb97X-D3 def2-SVP level for alcohols and the SDS and DBSA surfactants. According to the MEP analysis, the hydroxyl group position changed the electrostatic surface of the isomers of alcohols. With the exception of the hydroxyl group position at the alcohols and head regions of the surfactants, the distribution of the MEP was homogeneous for the tails in the molecules shown in Figure-6c, implying that there were specific sites which were available for nucleophilic and electrophilic attacks.

The electrostatic potential and conformations of GLY are shown in Figure 7. Figure 7A shows the MEP surfaces of the

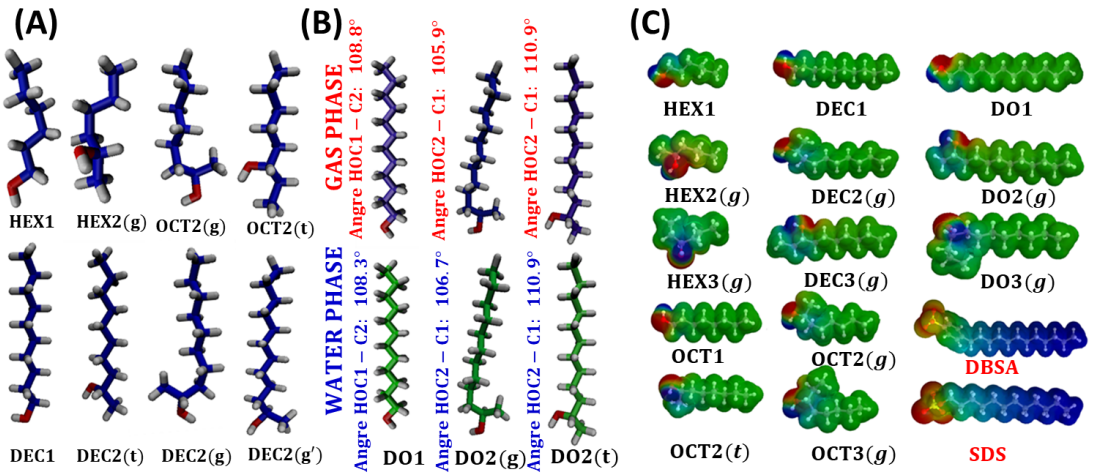

Figure 6. Structures and conformation of the alcohols and surfactants optimized with (A) DFT//B3LYP/6-31G (d) method; (B) Gas phase, DFT/B3LYP/6-31G and water phase, wb97X-D3 def2-SVP level; (C) Calculated (wb97X-D3 def2-SVP) Molecular Electrostatic Potential (MEP) of the alcohols isomers and surfactants.

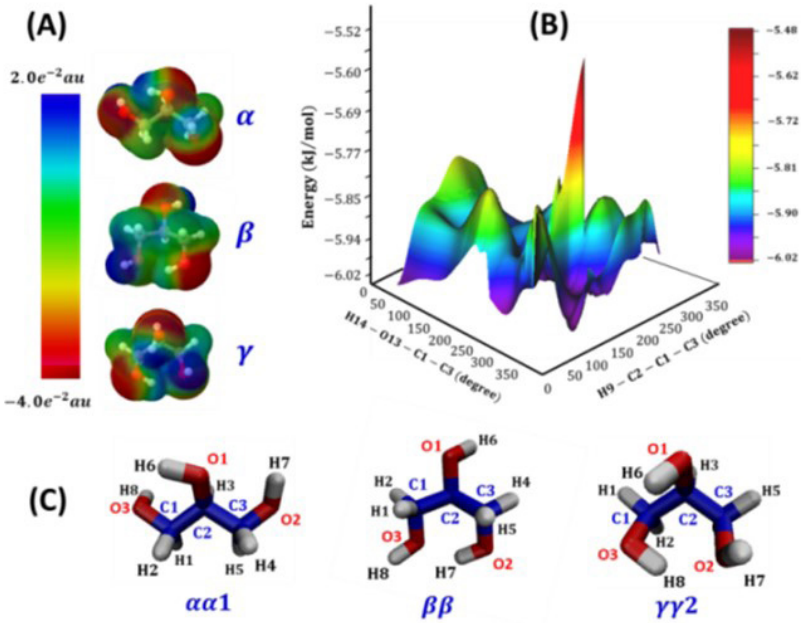

Figure 7. The conformations and properties of glycerol (A) The electrostatic potential is mapped onto the electron density surface with an isovalue of 0.0004 e-/au3 of α, β and γ conformations of glycerol; (B) The partial potential energy surface of glycerol calculated at a PM7 levels; (C) Computed structures αα1, ββ and γγ2 of glycerol.

α, β, and γ conformers of GLY and clearly indicates in the conformers has high electron density (red colour) changed with the geometry of hydroxyl group position. Significant differences were observed among the structures of the GLY conformers. The potential energy surface (Figure 7B) describes the relationship between the energy of a GLY molecule and its geometry as a function of dihedral D6 and D11 torsion angles The global minimum around dihedral (D6) and (D11) are relative of stable structures of GLY. For instance, most of the preferred conformers of GLY have two C_5 axes of symmetry hydrogen bonds in a gas phase, but in a liquid (water) phase, the hydrogen bonds of GLY appear to be weaker. The minimum energy was checked by the non-negative frequencies observed in the harmonic vibrational calculations. Here, the semi-empirical PM7 method was used to obtain an estimate of the variation in energy of the molecule as a function of the dihedral D6 and D11 torsion angles, which corresponded to the H9−C2−C1−C3 and H14−O13−C1−C3. The partial potential energy surface of GLY is shown in Figure 7B. Figure 7C illustrates the αα1, ββ, and γγ2 of the GLY optimised with DFT//B3LYP/6-31G(d) method. The solvation process weakened the hydrogen bonds of the

GLY, enlarged its potential surface and exists as an ensemble of many feasible local minima in water system. Glycerol consists of a blend of molecules with different conformations, and structural arrangements of hydroxymethyl (CH_2OH) and hydroxyl (OH) groups; indeed, there are 126 possible conformations in the gas, liquid, and solid states[28].

Molecular dynamics simulations were used to estimate the interfacial tensions for two immiscible liquid phases within the w/o reaction system. The w/o interfacial tension, g, was calculated using Equation 2, where L_z is the box length along the z-axis direction, P_{xx}, P_{yy}, P_{zz} are the normal and tangential components of the pressure tensor, and n is the number of interfaces in the system of the simulation box on the molecular dynamics[13-15].

$$\gamma(t)=\frac{1}{n}\int_0^{L_x}\left[P_{zz}(z,t)-\frac{P_{xx}(z,t)+P_{yy}(z,t)}{2}\right]dz \qquad (2)$$

To represent oil, we employed a mixture of DO1 and catalysts while the water was represented by an aqueous DBSA or SDS solution. The simulation box was a cubic cell with dimensions of $10\times10\times15$ nm^3 for systems where the organic phase was a pure component and $9\times9\times16$ nm^3 for systems where the organic phase consisted of 85/15% wt DO1/surfactant/catalyst (Figure 8). Initially, the oil model used in this study involved a mixture of DO1 and a surfactant in a 10:1 ratio, where the latter had a density of ~831 kg/m^3 at 298 K. The oil system was then mixed with the SPC and TIP3P water models to form two separate phases. Indeed, the density profile of this system showed that the water phase and the oil phase were perfectly separated. Based on the trajectory processing of this system simulation, an interfacial tension of 58.95 mN/m was obtained at 25 °C for the w/o liquid-liquid system. If the temperature was raised to 80 °C, the interfacial tension decreased to 56.54 mN/m. This was caused by the interaction of w/o, which was becoming stronger with rising temperatures. The results of the MD indicate that as the SDS or DBSA surface density increased, both the interfacial tension and the interfacial entropy increased: 25 °C, 28.30 mN/m and 353K, 18.86 mN/m for SDS.

The MD and *ab-initio* study reveal that in the GLY-αγ1 conformer the inter-molecular H-bonds led to the formation of bidentate ligands in the OH-groups of DO1 (Figure 8C), and for the intra- and inter-molecular H-bonds, five-member atoms rings in the αα and αγ conformers were formed. A six-atom ring coordination appeared in the γγ conformer. Angular molecular geometries were observed in the DO1, in which there was an important angle variation in 109° for 105° in the OH-groups. In the water/DO1 system HO−C bonding angles of 112° were observed for the dimers of DO1−HO----HO−DO1 and

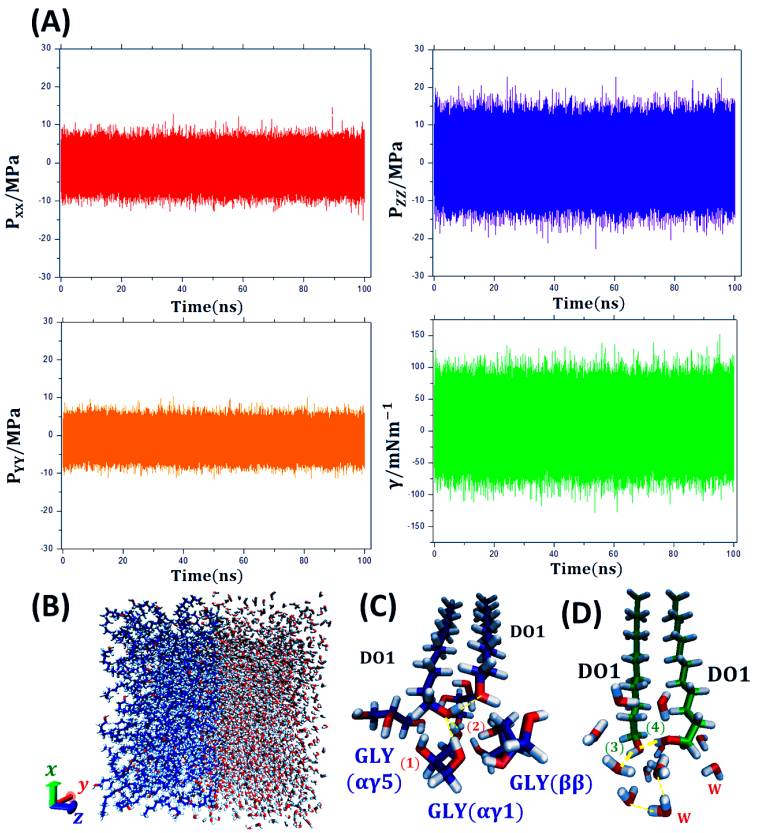

Figure 8. MD simulation details (A) diagonal elements of the pressure tensor P_{xx}, P_{yy} and P_{zz} and the resulting interfacial tension, γ, evaluated over the volume simulation box for the case biphasic system DO1/Water; (B) simulation box; (C) Snapshots obtained at 50 ns of the MD simulation for coordination geometries assumed by glycerol molecules upon H-bonding of dimer (tt) DO1 (D) Snapshot of H-bonding water OH-DO1 dimer (tt).

Table 6. Electronic properties calculated using DFT/B3LYP/6-31G.

Properties	DBSA	SDS	HEX1	OCT1	DEC1	DO1
HOMO (eV)	–1.575	–1.792	–7.435	–7.434	–7.364	–7.430
LUMO (eV)	2.512	2.736	0.848	0.806	0.753	0.834
E_g (eV)	4.087	4.528	8.283	8.240	8.117	8.264
χ (eV)	–0.469	–0.472	3.294	3.314	3.306	3.298
μ (eV)	0.469	0.472	–3.294	–3.314	–3.306	–3.298
η (eV)	2.044	2.264	4.142	4.120	4.059	4.132
s (eV)	0.245	0.221	0.121	0.121	0.123	0.121
ω (eV)	0.054	0.049	1.310	1.333	1.346	1.316
σ (eV)	0.489	0.442	0.241	0.243	0.246	0.242

angles of 113° appeared for DO1/water. Moreover, the water dipole was oriented toward the water bulk phase. The strong water/DO1 interaction was supported by the arrangements of surfaces for layers that were on top of eachother and which had a minimal surface roughness; the OH-groups and H_2O had overlapping densities in the *z*-direction. The most likely H-bonding configuration of DO1 derived from each molecule having one H-bond with water and two H-bonds with another molecule of DO1. Electronic properties play an important role in determining the efficacy of alcohol/GLY and surfactants as phase-forming components of biphasic systems. In the surfactants, the frontier molecular orbitals may predict how the charge transfers along the catalysis occur from liquid-liquid surface process or micelle. The reactivity parameters were based on the energies of the HOMO and those of the LUMO and Koopmans' theorem[41]. Table 6 shows the data collected for the quantum molecular descriptors quantum molecular descriptors: global hardness (η), electronegativity (χ), electronic chemical potential (μ), electrophilicity (ω) and softness chemistry (σ). The values of Eg imply a high or low stability or reactivity[42].

Therefore, both DBSA and SDS were considered stable compounds with values of 4.09 eV and 4.53 eV, respectively, but the alcohols were deemed stable with values ranging from 8.12−8.28 eV.

4. Conclusions

The polymerisation of PGs in an acidic medium was conducted successfully using an emulsion/micellar environment technique, and our theoretical studies (DFT and MD simulation) point to the influence of the conformation of alcohols and surfactants on the formation of micelles and their interface with influence on the catalytic process. We suggest that further studies are needed to better understand the effects of SDS and acid cocatalysts on the formation of hetero-ethers, alcohols, and homo-ethers.

5. Author's Contribution

- **Conceptualization –** Vadilson Malaquias dos Santos; Fabricio Uliana.
- **Data curation –** Vadilson Malaquias dos Santos; Fabricio Uliana; Rayanne Penha Wandenkolken Lima.
- **Formal analysis –** Vadilson Malaquias dos Santos; Fabricio Uliana; Rayanne Penha Wandenkolken Lima.
- **Funding acquisition –** NA.
- **Investigation –** Vadilson Malaquias dos Santos; Fabricio Uliana; Rayanne Penha Wandenkolken Lima.
- **Methodology –** NA.
- **Project administration –** Eloi Alves da Silva Filho.
- **Resources –** Vadilson Malaquias dos Santos; Fabricio Uliana; Rayanne Penha Wandenkolken Lima; Eloi Alves da Silva Filho.
- **Software –** Vadilson Malaquias dos Santos; Fabricio Uliana.
- **Supervision –** Eloi Alves da Silva Filho.
- **Validation –** Vadilson Malaquias dos Santos; Fabricio Uliana; Rayanne Penha Wandenkolken Lima.
- **Visualization –** Vadilson Malaquias dos Santos.
- **Writing – original draft –** Vadilson Malaquias dos Santos; Eloi Alves da Silva Filho.
- **Writing – review & editing –** Vadilson Malaquias dos Santos; Eloi Alves da Silva Filho.

6. Acknowledgements

The authors gratefully thanks to analysis by Nucleus of Competences in Petrochemical Chemistry (NCQP-UFES) for instrumentation.

7. References

1. Pouyan, P., Cherri, M., & Haag, R. (2022). Polyglycerols as multi-functional platforms: synthesis and biomedical applications. *Polymers*, *14*(13), 2684. http://dx.doi.org/10.3390/polym14132684. PMid:35808728.
2. Kuhn, R., Bryant, I. M., Jensch, R., & Böllmann, J. (2022). Applications of environmental nanotechnologies in remediation, wastewater treatment, drinking water treatment, and agriculture. *Applied Nanoscience*, *3*(1), 54-90. http://dx.doi.org/10.3390/applnano3010005.
3. Goyal, S., Hernández, N. B., & Cochran, E. W. (2021). An update on the future prospects of glycerol polymers. *Polymer International*, *70*(7), 911-917. http://dx.doi.org/10.1002/pi.6209.
4. Ebadipour, N., Paul, S., Katryniok, B., & Dumeignil, F. (2020). Alkaline-based catalysts for glycerol polymerization reaction:

a review. *Catalysts*, *10*(9), 1021. http://dx.doi.org/10.3390/catal10091021.

5. Liu, Y., Huang, K., Zhou, Y., Gou, D., & Shi, H. (2021). Hydrogen bonding and the structural properties of glycerol-water mixtures with a microwave field: a molecular dynamics study. *The Journal of Physical Chemistry B*, *125*(29), 8099-8106. http://dx.doi.org/10.1021/acs.jpcb.1c03232. PMid:34264668.
6. Shi, H., Fan, Z., Ponsinet, V., Sellier, R., Liu, H., Pera-Titus, M., & Clacens, J.-M. (2015). Glycerol/dodecanol double Pickering emulsions stabilized by polystyrene-grafted silica nanoparticles for interfacial catalysis. *ChemCatChem*, *7*(20), 3229-3233. http://dx.doi.org/10.1002/cctc.201500556.
7. Alashek, F., Keshe, M., & Alhassan, G. (2022). Preparation of glycerol derivatives by entered of glycerol in different chemical organic reactions: a review. *Results in Chemistry*, *4*, 100359. http://dx.doi.org/10.1016/j.rechem.2022.100359.
8. Piradashvili, K., Alexandrino, E. M., Wurm, F. R., & Landfester, K. (2016). Reactions and polymerizations at the liquid-liquid interface. *Chemical Reviews*, *116*(4), 2141-2169. http://dx.doi.org/10.1021/acs.chemrev.5b00567. PMid:26708780.
9. Amarasekara, A. S., Ali, S. R., Fernando, H., Sena, V., & Timofeeva, T. V. (2019). A comparison of homogeneous and heterogeneous Brønsted acid catalysts in the reactions of meso-erythritol with aldehyde/ketones. *SN Applied Sciences*, *1*(3), 212. http://dx.doi.org/10.1007/s42452-019-0226-9.
10. Li, X., Wu, L., Tang, Q., & Dong, J. (2017). Solvent-free acetalization of glycerol with n-octanal using combined Brønsted acid-surfactant catalyst. *Tenside, Surfactants, Detergents*, *54*(1), 54-63. http://dx.doi.org/10.3139/113.110480.
11. Toth, A., Schnedl, S., Painer, D., Siebenhofer, M., & Lux, S. (2019). Interfacial catalysis in biphasic carboxylic acid esterification with a nickel-based metallosurfactant. *ACS Sustainable Chemistry & Engineering*, *7*(22), 18547-18553. http://dx.doi.org/10.1021/acssuschemeng.9b04667.
12. Kralchevsky, P. A., Danov, K. D., Kolev, V. L., Broze, G., & Mehreteab, A. (2003). Effect of nonionic admixtures on the adsorption of ionic surfactants at fluid interfaces. 1. Sodium dodecyl sulfate and dodecanol. *Langmuir*, *19*(12), 5004-5018. http://dx.doi.org/10.1021/la0268496.
13. Burlatsky, S. F., Atrazhev, V. V., Dmitriev, D. V., Sultanov, V. I., Timokhina, E. N., Ugolkova, E. A., Tulyani, S., & Vincitore, A. (2013). Surface tension model for surfactant solutions at the critical micelle concentration. *Journal of Colloid and Interface Science*, *393*, 151-160. http://dx.doi.org/10.1016/j.jcis.2012.10.020. PMid:23153677.
14. Dong, W. (2021). Thermodynamics of interfaces extended to nanoscales by introducing integral and differential surface tensions. *Proceedings of the National Academy of Sciences of the United States of America*, *118*(3), e2019873118. http://dx.doi.org/10.1073/pnas.2019873118. PMid:33452136.
15. Kirkwood, J. G., & Buff, F. P. (1949). The statistical mechanical theory of surface tension. *The Journal of Chemical Physics*, *17*(3), 338-343. http://dx.doi.org/10.1063/1.1747248.
16. Pera-Titus, M., Leclercq, L., Clacens, J.-M., De Campo, F., & Nardello-Rataj, V. (2015). Pickering interfacial catalysis for biphasic systems: from emulsion design to green reactions. *Angewandte Chemie International Edition in English*, *54*(7), 2006-2021. http://dx.doi.org/10.1002/anie.201402069. PMid:25644631.
17. Gang, L., Xinzong, L., & Eli, W. (2007). Solvent-free esterification catalyzed by surfactant-combined catalysts at room temperature. *New Journal of Chemistry*, *31*(3), 348. http://dx.doi.org/10.1039/b615448d.
18. Pocheć, M., Krupka, K. M., Panek, J. J., Orzechowski, K., & Jezierska, A. (2022). Intermolecular interactions and spectroscopic signatures of the hydrogen-bonded system-n-octanol in experimental and theoretical studies. *Molecules (Basel, Switzerland)*, *27*(4), 1225. http://dx.doi.org/10.3390/molecules27041225. PMid:35209010.
19. Jindal, A., & Vasudevan, S. (2020). Hydrogen bonding in the liquid state of linear alcohols: molecular dynamics and thermodynamics. *The Journal of Physical Chemistry B*, *124*(17), 3548-3555. http://dx.doi.org/10.1021/acs.jpcb.0c01199. PMid:32242419.
20. Hanwell, M. D., Curtis, D. E., Lonie, D. C., Vandermeersch, T., Zurek, E., & Hutchison, G. R. (2012). Avogadro: an advanced semantic chemical editor, visualization, and analysis platform. *Journal of Cheminformatics*, *4*(1), 17. http://dx.doi.org/10.1186/1758-2946-4-17. PMid:22889332.
21. Stewart, J. J. P. (1990). MOPAC: a semiempirical molecular orbital program. *Journal of Computer-Aided Molecular Design*, *4*(1), 1-105. http://dx.doi.org/10.1007/BF00128336. PMid:2197373.
22. Neese, F., Wennmohs, F., Becker, U., & Riplinger, C. (2020). The ORCA quantum chemistry program package. *The Journal of Chemical Physics*, *152*(22), 224108. http://dx.doi.org/10.1063/5.0004608. PMid:32534543.
23. Dodda, L. S., Vaca, I. C., Tirado-Rives, J., & Jorgensen, W. L. (2017). LigParGen web server: an automatic OPLS-AA parameter generator for organic ligands. *Nucleic Acids Research*, *45*(W1), W331-W336. http://dx.doi.org/10.1093/nar/gkx312. PMid:28444340.
24. Silva, A. W. S., & Vranken, W. F. (2012). ACPYPE - AnteChamber PYthon Parser interfacE. *BMC Research Notes*, *5*(1), 367. http://dx.doi.org/10.1186/1756-0500-5-367. PMid:22824207.
25. Martínez, L., Andrade, R., Birgin, E. G., & Martínez, J. M. (2009). PACKMOL: a package for building initial configurations for molecular dynamics simulations. *Journal of Computational Chemistry*, *30*(13), 2157-2164. http://dx.doi.org/10.1002/jcc.21224. PMid:19229944.
26. Vassetti, D., Pagliai, M., & Procacci, P. (2019). Assessment of GAFF2 and OPLS-AA general force fields in combination with the water models TIP3P, SPCE, and OPC3 for the solvation free energy of druglike organic molecules. *Journal of Chemical Theory and Computation*, *15*(3), 1983-1995. http://dx.doi.org/10.1021/acs.jctc.8b01039. PMid:30694667.
27. Van Der Spoel, D., Lindahl, E., Hess, B., Groenhof, G., Mark, A. E., & Berendsen, H. J. C. (2005). GROMACS: fast, flexible, and free. *Journal of Computational Chemistry*, *26*(16), 1701-1718. http://dx.doi.org/10.1002/jcc.20291. PMid:16211538.
28. Valadbeigi, Y., & Farrokhpour, H. (2013). DFT study on the different oligomers of glycerol (n=1-4) in gas and aqueous phases. *Journal of the Korean Chemical Society*, *57*(6), 684-690. http://dx.doi.org/10.5012/jkcs.2013.57.6.684.
29. Gaudin, P., Jacquot, R., Marion, P., Pouilloux, Y., & Jérôme, F. (2011). Acid-catalyzed etherification of glycerol with long-alkyl-chain alcohols. *ChemSusChem*, *4*(6), 719-722. http://dx.doi.org/10.1002/cssc.201100129. PMid:21591271.
30. Fan, Z., Zhao, Y., Preda, F., Clacens, J.-M., Shi, H., Wang, L., Feng, X., & De Campo, F. (2015). Preparation of bio-based surfactants from glycerol and dodecanol by direct etherification. *Green Chemistry*, *17*(2), 882-892. http://dx.doi.org/10.1039/C4GC00818A.
31. Qian, J., Xu, J., & Zhang, J. (2011). SDS-catalyzed esterification process to synthesize ethyl chloroacetate. *Petroleum Science and Technology*, *29*(5), 462-467. http://dx.doi.org/10.1080/10916461003610405.
32. Sivaiah, M. V., Robles-Manuel, S., Valange, S., & Barrault, J. (2012). Recent developments in acid and base-catalyzed etherification of glycerol to polyglycerols. *Catalysis Today*, *198*(1), 305-313. http://dx.doi.org/10.1016/j.cattod.2012.04.073.

33. Szeląg, H., & Sadecka, E. (2009). Influence of sodium dodecyl sulfate presence on esterification of propylene glycol with lauric acid. *Industrial & Engineering Chemistry Research*, *48*(18), 8313-8319. http://dx.doi.org/10.1021/ie8019449.

34. Kirby, F., Nieuwelink, A.-E., Kuipers, B. W. M., Kaiser, A., Bruijnincx, P. C. A., & Weckhuysen, B. M. (2015). CaO as drop-in colloidal catalysts for the synthesis of higher polyglycerols. *Chemistry (Weinheim an der Bergstrasse, Germany)*, *21*(13), 5101-5109. http://dx.doi.org/10.1002/chem.201405906. PMid:25684403.

35. Al-Soufi, W., & Novo, M. (2021). A surfactant concentration model for the systematic determination of the critical micellar concentration and the transition width. *Molecules (Basel, Switzerland)*, *26*(17), 5339. http://dx.doi.org/10.3390/molecules26175339. PMid:34500770.

36. Shah, S. S., Jamroz, N. U., & Sharif, Q. M. (2001). Micellization parameters and electrostatic interactions in micellar solution of sodium dodecyl sulfate (SDS) at different temperatures. *Colloids and Surfaces. A, Physicochemical and Engineering Aspects*, *178*(1–3), 199-206. http://dx.doi.org/10.1016/S0927-7757(00)00697-X.

37. El-Dossoki, F. I., Gomaa, E. A., & Hamza, O. K. (2019). Solvation thermodynamic parameters for sodium dodecyl sulfate (SDS) and sodium lauryl ether sulfate (SLES) surfactants in aqueous and alcoholic-aqueous solvents. *SN Applied Sciences*, *1*(8), 933. http://dx.doi.org/10.1007/s42452-019-0974-6.

38. Zana, R. (1995). Aqueous surfactant-alcohol systems: a review. *Advances in Colloid and Interface Science*, *57*, 1-64. http://dx.doi.org/10.1016/0001-8686(95)00235-I.

39. Nguyen, K. T., & Nguyen, A. V. (2019). New evidence of head-to-tail complex formation of SDS-DOH mixtures adsorbed at the air-water interface as revealed by vibrational sum frequency generation spectroscopy and isotope labelling. *Langmuir*, *35*(14), 4825-4833. http://dx.doi.org/10.1021/acs.langmuir.8b04213. PMid:30866624.

40. Chelli, R., Gervasio, F. L., Gellini, C., Procacci, P., Cardini, G., & Schettino, V. (2000). Density functional calculation of structural and vibrational properties of glycerol. *The Journal of Physical Chemistry A*, *104*(22), 5351-5357. http://dx.doi.org/10.1021/jp0000883.

41. Vargas, R., Garza, J., & Cedillo, A. (2005). Koopmans-like approximation in the Kohn-Sham method and the impact of the frozen core approximation on the computation of the reactivity parameters of the density functional theory. *The Journal of Physical Chemistry A*, *109*(39), 8880-8892. http://dx.doi.org/10.1021/jp052111w. PMid:16834292.

42. Yu, J., Su, N. Q., & Yang, W. (2022). Describing chemical reactivity with frontier molecular orbitalets. *JACS Au*, *2*(6), 1383-1394. http://dx.doi.org/10.1021/jacsau.2c00085. PMid:35783161.

Received: Jan. 24, 2023
Revised: June 28, 2023
Accepted: Dec. 11, 2023